Benchmark case: Axial Fan Measurements

All experimental investigations were made in a standardized inlet test chamber according to ISO 5801, see figure 2. The test chamber was built as an anechoic chamber with absorbing walls, ceiling and floor, to enable aeroacoustic measurements. The fan's operating point was carefully adjusted with the butterfly damper (decrease volumetric flow) or the auxiliary fan (increase volumetric flow). The volumetric flow was determined with a standardized bellmouth inlet, see figure 2. The fan was installed in a short duct with an inlet nozzle on the suction side and a diffusor on the pressure side to resemble a realistic test setup, see figure 1.

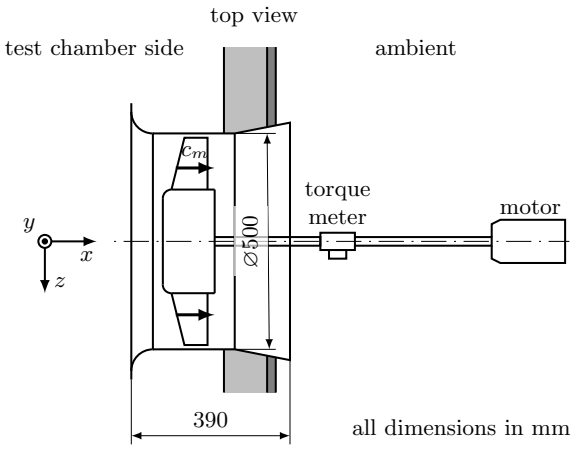

Figure 1: Experimental setup - detail view.

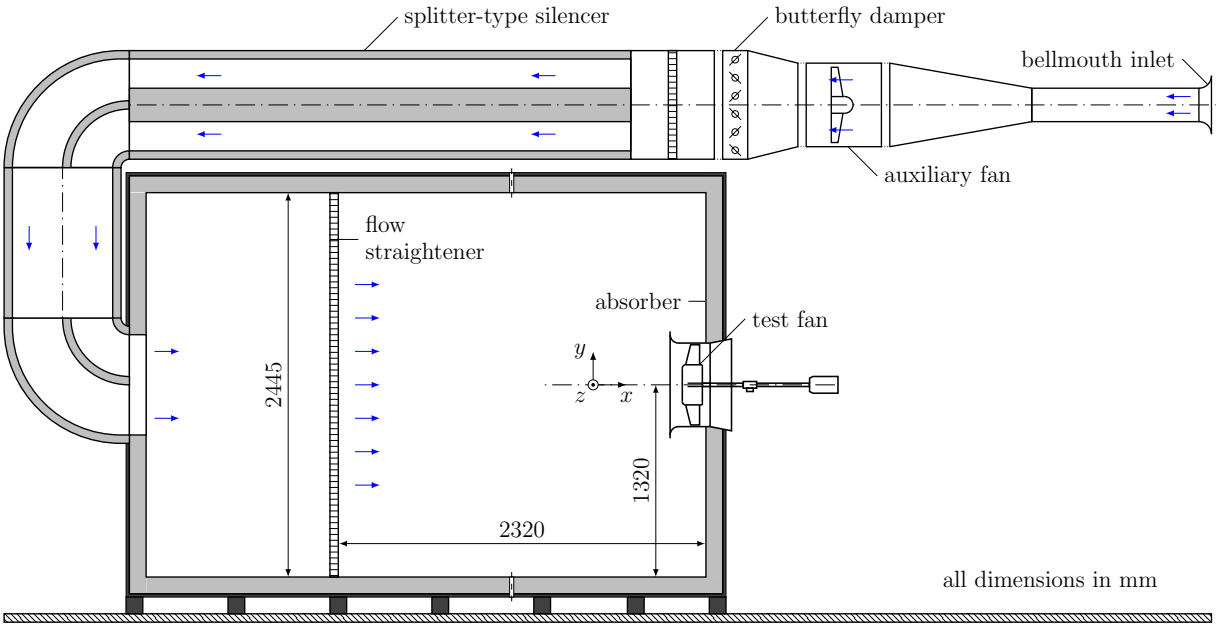

Figure 2: Standardized inlet test chamber.

The fan was driven by a motor outside the duct. Torque and rotational speed were measured with a precision torque meter, see figure 1.

Measurement details

Information on the used measurement equipment and measuring times are shown in this sections. A detailed description of the experimental setup and the measurement positions is given in [1].

LDA	
LDA system	2-component LDA probe, type 2D FiberFlow (Dantec Dynamics) BSA P80 burst spectrum analyzer (Dantec Dynamics) BSA Flow software v5.20 (Dantec Dynamics)
Measurement time	12 min or 2.5×10^6 samples per position
Wall pressure fluctuations	
Type	differential pressure transducers XCS-093-1psi D (Kulite Semiconductor Products
Measurement time	30 s with a sampling frequency of 48 kHz
Microphones	
Type	1/2 inch free-field microphones 4189-L-001 (Brüel & Kjær
Measurement time	30 s with a sampling frequency of 48 kHz
Microphone array microphones	
Type	1/4 inch array microphones 40PH-Sx (G.R.A.S. Sound & Vibration)
Measurement time	30 s with a sampling frequency of 48 kHz

References

[1] Zenger, F., Junger, C., Kaltenbacher, M., and Becker, S., "A Benchmark Case for Aerodynamics and Aeroacoustics of a Low Pressure Axial Fan," SAE Technical Paper 2016-01-1805, 2016, doi: 10.4271/2016-01-1805.

[2] International Organization for Standardization, "ISO 5801:2007 Industrial Fans - Performance Testing Using Standardized Airways", 2007.

Results

This section includes the results for the fan aerodynamic and acoustic characteristic curve, flow field on the suction and pressure side, wall pressure fluctuations and sound field.

Fan characteristic curve

The aerodynamic characteristic curve is shown in figure 3.

The fan reaches a maximum volumetric flow of $\dot{V} \approx 2.1\,\mathrm{m\,s^{-1}}$ for $\Delta p_{\mathrm{ts}} = 0$ and a maximum pressure difference of $\Delta p_{\mathrm{ts}} = 250\,\mathrm{Pa}$ for $\dot{V} \approx 0.2\,\mathrm{m\,s^{-1}}$. The total-to-static efficiency is 53 % at the design volumetric flow of $\dot{V} = 1.4\,\mathrm{m\,s^{-1}}$.

Figure 4 shows the acoustic characteristic curve of fan N1UG. At the design volumetric flow, the overall sound power level is $L_{\mathrm{W}} = 87.3\,\mathrm{dB}$. Stall onset at lower volumetric flows can be detected by the rise in L_{W} at $1.1\,\mathrm{m^3\,s^{-1}}$ with a maximum of $L_{\mathrm{W}} = 93\,\mathrm{dB}$ at $\dot{V} = 1\,\mathrm{m\,s^{-1}}$.

Flow field

Figure 5 shows the time averaged values of the meridional velocity on the suction and pressure side for a volumetric flow of $1.4\,\mathrm{m^3\,s^{-1}}$.

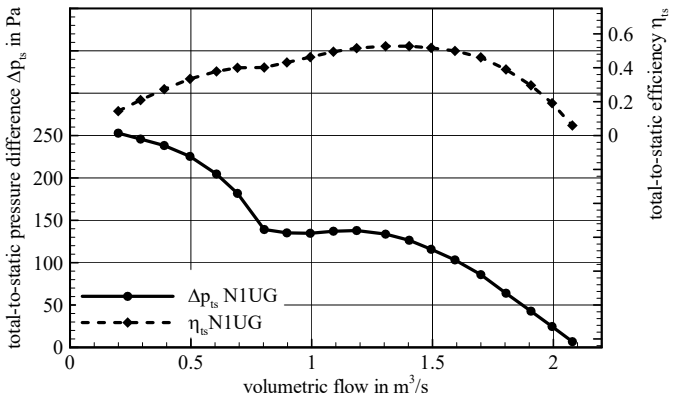

Figure 3: Fan aerodynamic characteristic curve.

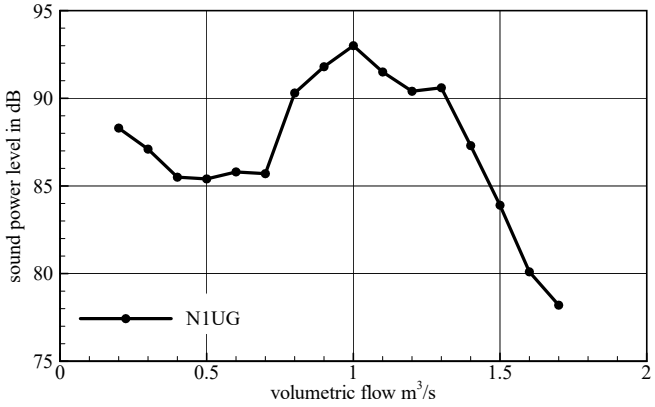

Figure 4: Fan acoustic characteristic curve.

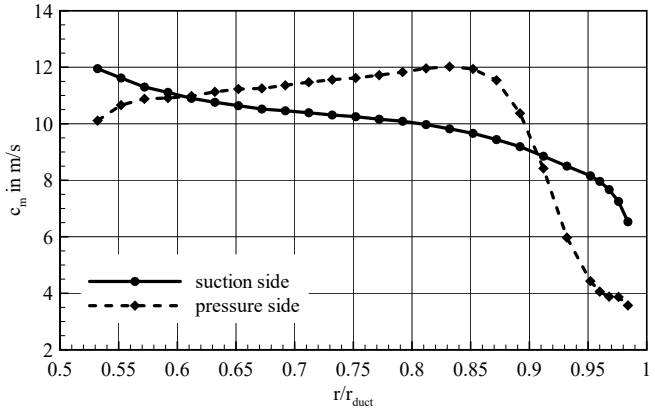

Figure 5: Time averaged values of meridional velocity on suction and pressure side.

On the suction side, the meridional flow is accelerated around the hub at $r/r_{\mathrm{duct}} = 0.5$ and then decreased towards the duct wall at $r/r_{\mathrm{duct}} = 1$. On the pressure side, the peak velocity is at $r/r_{\mathrm{duct}} = 0.84$ with $12\,\mathrm{m\,s^{-1}}$. Towards the hub, it decreases to $10\,\mathrm{m\,s^{-1}}$ and towards the duct wall to $3.5\,\mathrm{m\,s^{-1}}$.

Figure 6a shows the ensemble averaged values for meridional velocity c_m (contour) and circumferential velocity c_θ and radial velocity c_r (vector field) on the suction side with fan N1UG in the background. Rotational direction is clockwise.

Corresponding to figure 5, the meridional velocity decreases from hub to tip. The maximum is reached during the blade passage near the hub. The circumferential velocity is also maximal near the hub, short after the blade passage. Near the tip, a small region with flow against the rotational direction during the blade passage can be observed. The radial velocity shows high values during the blade passage at the midspan region.

Accordingly, figure 6b shows the ensemble averaged values for the pressure side. Here, the meridional velocity c_m has the highest values in between two blade passages. Due to the motion of the fan, a circumferential component is superimposed on the pressure side. The values are small in the same region as with high meridional velocity. Radial velocity is rather constant, only near the hub, a region with negative values can be observed.

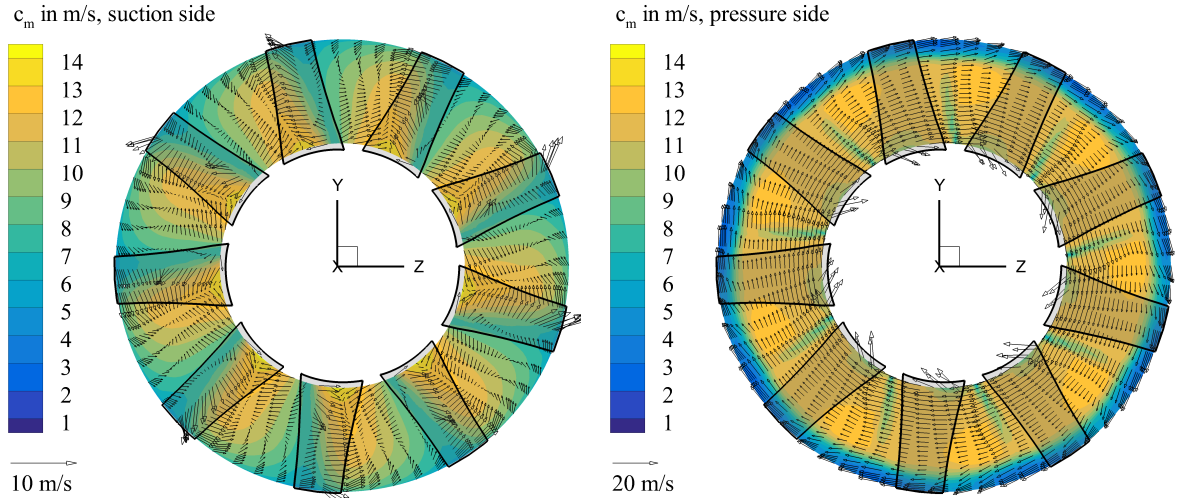

a Suction side: ensemble averaged meridional velocity c_m.

b Pressure side: ensemble averaged circumferential velocity c_θ.

Figure 6: Ensemble averaged velocity values.

The ensemble averaged turbulent kinetic energy on the suction and pressure side is shown in figures 7a and 7b. On the suction side, values are low, except during the blade passage where the turbulent kinetic energy reaches values of $k = 35\,\mathrm{m^2/s^2}$. On the pressure side, turbulent kinetic energy is high at the blade tips and at the hub region.

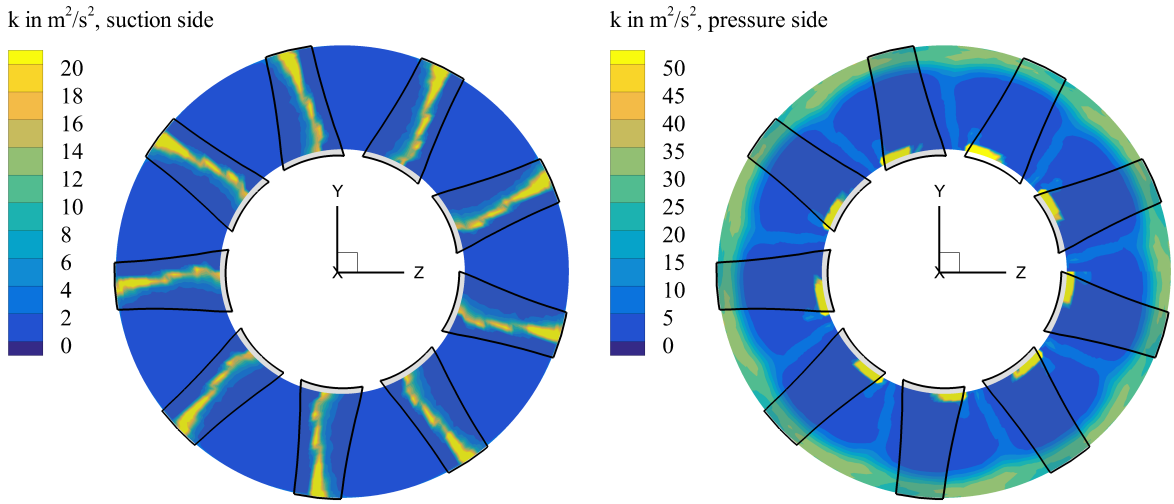

a Suction side: ensemble averaged turbulent kinetic energy k.

b Pressure side: ensemble averaged turbulent kinetic energy k.

Figure 7: Turbulent kinetic energy.

Wall pressure fluctuations

Spectra of wall pressure fluctuations (superposition of acoustic and hydrodynamic fluctuations) for selected transducers are shown in figure 8. Note that y-axis values are in dB.

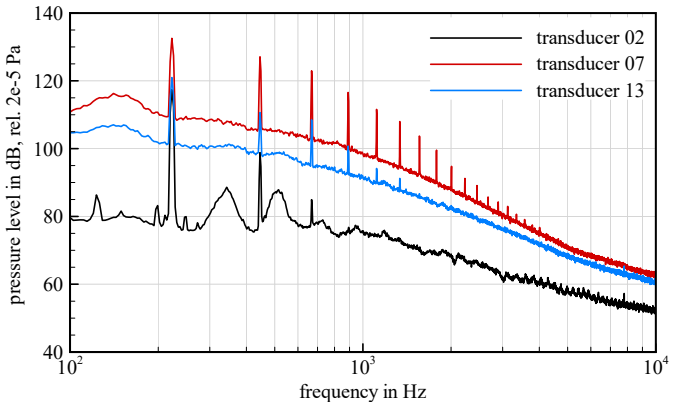

Figure 8: Spectra of wall pressure fluctuations.

Tonal components can mainly be seen at the blade passing frequency (BPF) at 225 Hz and harmonics. The curve for transducer 2 shows the highest broadband values, being axially positioned very close to the blade tip during the blade passage. Elevations can also be observed at 338 Hz ($1.5 \cdot$ BPF) and $1.5 \cdot 338\,\text{Hz} = 507\,\text{Hz}$. This effect does also occur in the sound power spectrum.

Sound field

The sound power spectrum, calculated from seven 1/2 inch free-field microphones is shown in figure 9. Tonal components can be seen at the BPF (225 Hz) and harmonics. Additional tonal components in the range from 7 kHz to 8.5 kHz are caused by the frequency converter of the drive motor. Similar to the spectrum of wall pressure fluctuations of transducer 2, subharmonic peaks can be observed at 338 Hz and 507 Hz. The amplitude of the highest peak is even above the amplitude of the BPF, suggesting a dominant effect. It is expected that this is caused by an interaction of the gap flow with the fan blades.

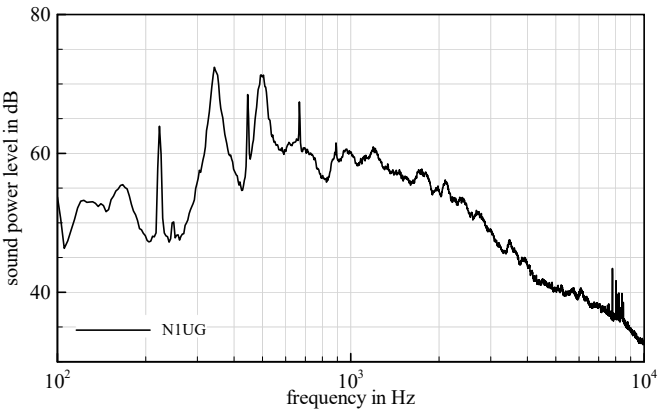

Figure 9: Sound Power Spectra.

Beamforming results for 2 kHz, 4 kHz and 5 kHz third-octave band are displayed in figures 10 to 12. On low pressure axial fans, leading edge noise is expected to be prevailing in the low-frequency region, whereas trailing edge noise is mainly anticipated in the high-frequency region. Futhermore, more sound sources are anticipated at the blade tip, as there is a higher circumferential velocity and consequently a higher Mach number than at the hub region. Looking at the sound map at 2 kHz, this can be confirmed, as sound sources are mainly located at the leading edge and at the blade tip (with high circumferential velocity). At 4 kHz, sound sources are distributed over the whole region from leading to trailing edge. Hence the transition from leading to trailing edge noise takes place in this frequency band. At 5 kHz, sound sources are more dominant on the trailing edge than on the leading edge.

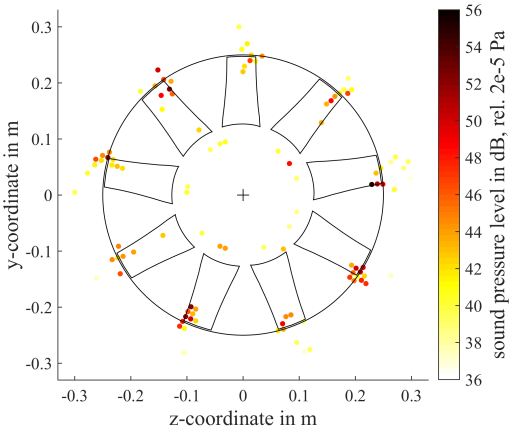

Figure 10: Sound map, 2 kHz third-octave band.

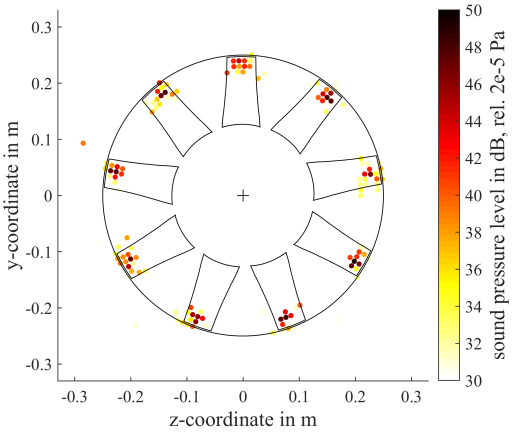

Figure 11: Sound map, 4 kHz third-octave band.

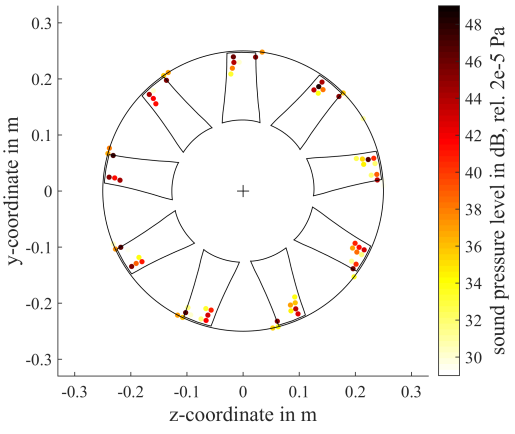

Figure 12: Sound map, 5 kHz third-octave band.